Hyperfine Averaging by Dynamic Decoupling in a Multi-Ion Lutetium Clock

R. Kaewuam,[1] T. R. Tan,[1,2] K. J. Arnold,[1] S. R. Chanu,[1] Zhiqiang Zhang,[1] and M. D. Barrett[1,2,*]
[1]Centre for Quantum Technologies, National University of Singapore, 3 Science Drive 2, 117543 Singapore
[2]Department of Physics, National University of Singapore, 2 Science Drive 3, 117551 Singapore

(Received 11 October 2019; accepted 3 February 2020; published 26 February 2020)

We propose and experimentally demonstrate a scheme that realizes hyperfine averaging during a Ramsey interrogation of a clock transition. The method eliminates the need to average over multiple optical transitions, reduces the sensitivity of the clock to its environment, and reduces inhomogeneous broadening in a multi-ion clock. The method is compatible with autobalanced Ramsey spectroscopy, which facilitates the elimination of residual shifts due to imperfect implementation and ac stark shifts from the optical probe. We demonstrate the scheme using correlation spectroscopy of the $^1S_0 \leftrightarrow {}^3D_1$ clock transition in a three-ion Lu^+ clock. From the demonstration we are able to provide a measurement of the $^3D_1$ quadrupole moment, $\Theta(^3D_1) = 0.634(9)ea_0^2$.

DOI: 10.1103/PhysRevLett.124.083202

Optical atomic clocks have seen rapid advances over the last decade with a number of systems now reaching fractional uncertainties near to $\sim 10^{-18}$ [1–5]. Singly ionized lutetium ($^{176}Lu^+$) is a relatively new clock candidate with a number of attractive features for clock applications [6–8]. It provides three independent clock transitions allowing consistency checks on error budgets through frequency comparisons within the one system. Two of the transitions allow long interrogation times relevant to current state-of-the-art lasers, and have atomic properties relevant to clock performance that compare favorably to other leading clock candidates [7]. As with other ion-based clocks, single-ion operation limits fractional instability to $\sim 10^{-15}/\sqrt{\tau}$, for which averaging times (τ) of several days or even weeks are required to reach 10^{-18} resolution [9]. For this reason, multi-ion clock implementations are of interest [8,10–12]. Recent work illustrated the feasibility of a $^{176}Lu^+$ multi-ion approach by demonstrating suppression of inhomogeneous broadening to the level of 10^{-17} and the potential for clock interrogation times $\gtrsim 10$ s. However, averaging over excited hyperfine states is still required to make full use of the advantages $^{176}Lu^+$ has to offer [6].

All optical clock implementations use some form of averaging to cancel various systematic shifts, be it averaging over Zeeman pairs [13], hyperfine states [6], or orthogonal orientations of the magnetic field [14]. In a multi-ion crystal, individual systematic shifts become a source of inhomogeneous broadening, which can diminish the efficacy of averaging particularly for long interrogation times; as the interrogation time increases, individual shifts become increasingly resolved, which distorts the line shape of a multi-ion spectroscopy signal and shifts the line center away from the mean. Hence, broadening mechanisms must be well characterized and controlled, which can be a significant challenge in an ensemble of ions. Nevertheless, progress towards multi-ion operation has been made: precision engineering of the ion trap has allowed the control of excess-micromotion (EMM) shifts to the 10^{-19} level over millimeter length scales [15], precise alignment of the magnetic field has demonstrated the suppression of tensor shifts [8], and dynamic decoupling during interrogation has also demonstrated suppression of inhomogeneous broadening [12].

Dynamic decoupling is an attractive approach to suppressing inhomogeneous broadening, as it also reduces the sensitivity of the clock frequency to electromagnetic fields, and simplifies the averaging by eliminating the need to probe multiple transitions. However, the recent demonstration in $^{88}Sr^+$ [12] made use of the uniform spacing between Zeeman sublevels, and is not directly applicable to averaging across hyperfine states in the case of $^{176}Lu^+$. Instead we use a simple scheme in which the atomic coherence is transferred between hyperfine states during a Ramsey interrogation so that each upper state is sampled for an equal duration of time. This effectively implements hyperfine averaging within a single interrogation sequence and can be interpreted as a form of dynamic decoupling.

Consider a Ramsey interrogation of the $^1S_0$ to $^3D_1$ transition using the sequence shown in Fig. 1, in which microwave transitions within the interrogation time are used to effect hyperfine averaging. The ground state and upper $m = 0$ states are denoted $|g\rangle$ and $|F\rangle$, respectively, with $F = \{6, 7, 8\}$. A laser of frequency ω_L drives the optical transition $|g\rangle \leftrightarrow |7\rangle$ with a coupling strength Ω_L. Frequencies and coupling strengths of the applied microwave fields are denoted ω_k' and Ω_k, respectively, with $k = 1$ corresponding to the transition $|8\rangle \leftrightarrow |7\rangle$ and $k = 2$ to $|7\rangle \leftrightarrow |6\rangle$. Although Fig. 1 shows a sequence relevant to

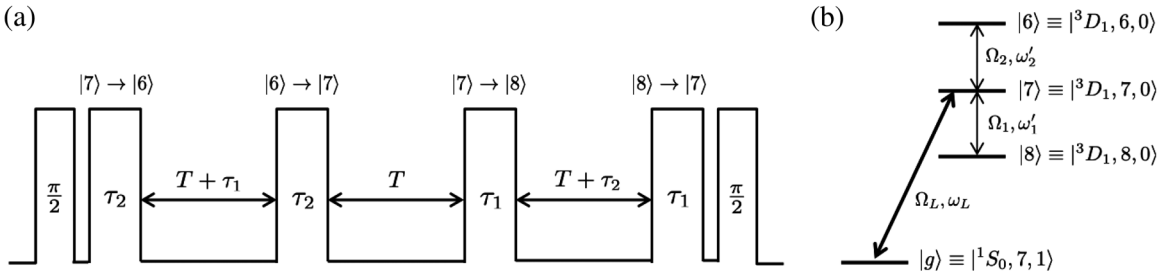

FIG. 1. Dynamic decoupling used to effect hyperfine averaging. (a) Pulse sequence used. The $\pi/2$ pulses provide Ramsey spectroscopy of the $|g\rangle \leftrightarrow |7\rangle$ transition. Pulses labeled τ_1 and τ_2 are microwave π pulses driving $|8\rangle \leftrightarrow |7\rangle$ and $|6\rangle \leftrightarrow |7\rangle$, respectively. (b) Level scheme for the states involved: Applied microwave fields have angular frequencies $\omega_1 = 2\pi \times 10.49\,\mathrm{GHz}$ and $\omega_2 = 2\pi \times 11.29\,\mathrm{GHz}$.

the optical addressing of $|g\rangle \leftrightarrow |7\rangle$, any upper state, $|F\rangle$, may be used with an appropriate reordering of the microwave pulses. In the general case, the Hamiltonian in the interaction picture is

$$\begin{aligned} H_I = {} & \frac{\Omega_L}{2}(e^{-i(\omega_L-\omega_{\bar{F}})t}|\bar{F}\rangle\langle g| + e^{i(\omega_L-\omega_{\bar{F}})t}|g\rangle\langle\bar{F}|) \\ & + \frac{\Omega_2}{2}(e^{-i\Delta_2 t}|6\rangle\langle 7| + e^{i\Delta_2 t}|7\rangle\langle 6|) \\ & + \frac{\Omega_1}{2}(e^{-i\Delta_1 t}|7\rangle\langle 8| + e^{i\Delta_1 t}|8\rangle\langle 7|), \end{aligned} \tag{1}$$

where we have kept only near resonant terms and used $\bar{F}$ to denote the specific hyperfine state addressed by the laser. Upper state energies $\hbar\omega_F$ are taken relative to the zero-point energy of the ground state, and $\Delta_k = \omega_k' - \omega_k$ are the microwave detunings relative to their respective resonances $\omega_1 = \omega_7 - \omega_8$ and $\omega_2 = \omega_6 - \omega_7$.

In what follows, it is convenient to introduce the signed frequency combinations,

$$\bar{\omega}_6 = \frac{2\omega_2 + \omega_1}{3}, \quad \bar{\omega}_7 = -\frac{\omega_2 - \omega_1}{3}, \quad \bar{\omega}_8 = -\frac{2\omega_1 + \omega_2}{3},$$

and counterparts, $\bar{\omega}_F'$, defined in a similar way with ω_k' replacing ω_k. The frequencies $\bar{\omega}_F$ are the offsets of a given level from the hyperfine averaged frequency, ω_0. That is,

$$\omega_0 = \frac{\omega_6 + \omega_7 + \omega_8}{3} = \omega_F - \bar{\omega}_F. \tag{2}$$

With these definitions at hand, we transform Eq. (1) to a rotating frame using $U = e^{iH_0 t}$ where

$$H_0 = -\delta|g\rangle\langle g| + \sum_F \Delta_F |F\rangle\langle F|, \tag{3}$$

with the parameters δ and Δ_F conveniently set to

$$\Delta_F = \bar{\omega}_F' - \bar{\omega}_F = \omega_0 + \bar{\omega}_F' - \omega_F, \tag{4}$$

and

$$\delta = \omega_L - \omega_{\bar{F}} - \Delta_{\bar{F}} = \omega_L - \bar{\omega}_{\bar{F}}' - \omega_0. \tag{5}$$

In the rotating frame we then have

$$\begin{aligned} H = {} & \delta|g\rangle\langle g| - \sum_F \Delta_F |F\rangle\langle F| + \frac{\Omega_L}{2}(|\bar{F}\rangle\langle g| + |g\rangle\langle\bar{F}|) \\ & + \frac{\Omega_2}{2}(|6\rangle\langle 7| + |7\rangle\langle 6|) + \frac{\Omega_1}{2}(|7\rangle\langle 8| + |8\rangle\langle 7|). \end{aligned} \tag{6}$$

We can now consider the phase accumulated in a Ramsey sequence including two microwave π pulses from both sources as required to cycle through all states. We denote the microwave π-pulse times by $\tau_k = \pi/(2\Omega_k)$ and consider the Ramsey times of $T + \tau_1$, T, and $T + \tau_2$ associated with $|6\rangle$, $|7\rangle$, and $|8\rangle$, respectively. Starting from the initial state $|\psi_0\rangle = |g\rangle - i|\bar{F}\rangle$ arising from the first optical Ramsey pulse, the ground state accumulates a phase $-3\delta(T + \tau_1 + \tau_2)$ and the upper state accumulates

$$T\sum_F \Delta_F + \tau_1\Delta_6 + \tau_2\Delta_8 + (\Delta_8 + \Delta_7)\tau_1 + (\Delta_7 + \Delta_6)\tau_2, \tag{7}$$

where the first three terms originate from the Ramsey time in each upper state, and the remaining terms originate from the π pulses. Since $\sum_F \Delta_F = 0$, the phase shift on the upper state is zero, and the central Ramsey fringe satisfies $\delta = 0$. From the definition of δ, this is the shift relative to $\omega_0 + \bar{\omega}_{\bar{F}}'$. Down-shifting the laser by the well defined microwave offset $\bar{\omega}_{\bar{F}}'$, then gives the hyperfine averaged frequency, ω_0, free of any tensor shifts, leading quadratic Zeeman shifts [6], and any associated inhomogeneous broadening. We emphasize that the clock frequency is a combination of the optical and microwave frequencies $\omega_L - \bar{\omega}_{\bar{F}}'$ and that the Ramsey interrogation sequence we have described detects any offset of this from the hyperfine averaged frequency.

To understand the phase evolution during the microwave pulse, consider the two level system with Hamiltonian

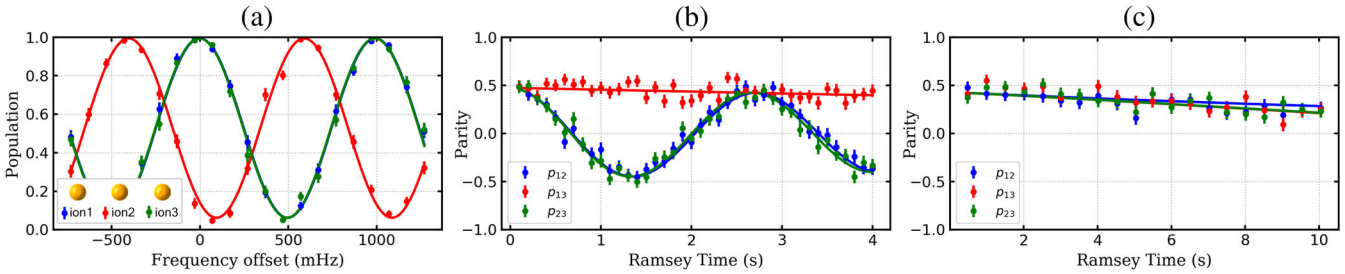

FIG. 2. (a) Microwave Ramsey spectroscopy of the $|{}^3D_1, 8, 0\rangle \leftrightarrow |{}^3D_1, 7, 0\rangle$ transition using a 1 s Ramsey time. Frequencies on the horizontal axes are relative to the measured hyperfine splitting of ~10.49 GHz of the outer ions (ions 1 and 3). The center fringe for the middle ion (ion 2) is offset by ≈0.6 Hz. (b) Correlation spectroscopy on the $|{}^1S_0, 7, 1\rangle \leftrightarrow |{}^3D_1, 7, 0\rangle$ transition without dynamic decoupling. (c) Correlation spectroscopy on the $|{}^1S_0, 7, 1\rangle \leftrightarrow |{}^3D_1, 7, 0\rangle$ transition using the decoupling sequence shown in Fig. 1 with microwave π times $\tau_1 = \tau_2 = 10$ ms and $\tau = 5$ ms for the optical $\pi/2$ pulses.

$$\begin{pmatrix} \delta_1 & \Omega \\ \Omega & \delta_2 \end{pmatrix} = \begin{pmatrix} \frac{\delta_1+\delta_2}{2} & 0 \\ 0 & \frac{\delta_1+\delta_2}{2} \end{pmatrix} + \begin{pmatrix} \frac{\delta_1-\delta_2}{2} & \Omega \\ \Omega & -\frac{\delta_1-\delta_2}{2} \end{pmatrix}.$$

As the first term clearly commutes with the second, the corresponding unitary evolution factors, with the first term giving rise to a global phase. In a conventional Ramsey interrogation a global phase has no influence on the spectroscopy. However, for microwave pulses used within the Ramsey sequence, the phase only applies to the upper states and hence to the optical phase being tracked by the superposition. Intuitively, the contribution is simply the average from each: that arising from $|6\rangle$ and $|7\rangle$ for one pulse, and from $|7\rangle$ and $|8\rangle$ for the other. For all pulses used, $|7\rangle$ is over-represented or, equivalently, $|6\rangle$ and $|8\rangle$ under-represented, which is compensated by the appropriate increase the Ramsey times associated with $|6\rangle$ and $|8\rangle$.

To demonstrate the method, we use a combination of microwave and optical spectroscopy in a three-ion optical clock as described in our recent work [8]. We first align the magnetic field along the trap axis, which maximizes inhomogeneous broadening between the ions. We then show that the broadening is eliminated by the decoupling protocol.

The magnetic field is aligned with respect to a π-polarized optical pumping beam, which addresses the ${}^3D_1$, $F = 7$ to ${}^3P_0$, $F' = 7$ transition at 646 nm. Maximizing depumping times out of $|7\rangle$ by the optical pumping beam ensures that the magnetic field is well aligned to the laser polarization, which geometry constrains to about $\pm 5°$ with respect to the crystal axis. However the actual angle is not crucial for our demonstration.

Ramsey spectroscopy of the $|8\rangle \leftrightarrow |7\rangle$ transition is carried out to characterize the broadening arising from differential tensor shifts between the ions. As in a previous work [8], the most significant contribution is due to the coupling of the quadrupole moment to the Coulomb field from neighboring ions, with axial micromotion arising from the end cap design of the trap contributing at the 1% level from the associated ac Stark shift. Provided micromotion is well compensated for the middle ion, both effects shift the outer ions equally with respect to the middle ion as is evident from the data shown in Fig. 2(a).

To demonstrate the averaging protocol, we use correlation spectroscopy of the $|g\rangle \equiv |{}^1S_0, 7, 1\rangle \leftrightarrow |7\rangle$ transition both with and without decoupling. As discussed elsewhere [8,16,17], correlation spectroscopy enables frequency comparison between pairs of ions beyond the radiation's coherence time. Under the assumption of a uniform distribution of phases, the expectation value of the parity operator $p_{ij} = \langle \sigma_{z,i} \sigma_{z,j} \rangle$ is

$$p_{ij} = \frac{p_c}{2} \cos(2\pi \Delta f_{ij} T_R), \tag{8}$$

where p_c characterizes the loss of relative coherence between the two atomic oscillators under investigation, Δf_{ij} is the difference in their resonant transition frequencies, and T_R is total Ramsey time.

Results of correlation spectroscopy without decoupling is shown in Fig. 2(b). As expected, there is an oscillation in the correlation signals p_{12} and p_{23} and no significant oscillation in p_{13}. The differential tensor shift between ions inferred from the correlation signals is 589.0(3.2) mHz which is consistent with 592.2(4.5) mHz measured from the microwave Ramsey spectroscopy [Fig. 1(a)]. The small frequency difference in the correlation signals p_{12} and p_{23} is due to a 113 μT/m magnetic field gradient and the ~3.4 kHz/mT Zeeman sensitivity of $|g\rangle$. The gradient was independently measured via microwave correlation spectroscopy of the $|{}^3D_1, 6, -1\rangle \leftrightarrow |7\rangle$ transition as demonstrated in [8]. With the decoupling sequence shown in Fig. 1, oscillations in p_{12} and p_{23} are no longer present as shown in Fig. 2(c). As seen in our previous work [8], there is a noticeable decay that cannot be explained by the expected frequency differences from micromotion and magnetic field gradients. To allow for possible dephasing, we fit the data to Eq. (8) using $p_c = p_0^2 \exp(-t/T_c)$, with p_0 and T_c as free parameters, and Δf_{ij} set to the measured values. This gives $p_0 = 0.93(2)$, and a dephasing time of

$T_c = 24(3)$ s consistent with the $T_c = 27(6)$ s found in previous work [8].

Due consideration should be given to the microwave π-pulse times used. If the pulses are too long, they could resolve the shifts of individual ions. This is unlikely to be a problem for practical clock operation, as the magnetic field would be first aligned to suppress inhomogeneous broadening as demonstrated in [8]. With shorter pulse times, one must account for ac Zeeman shifts arising from off-resonant microwave couplings, particularly from the $\sigma^{\pm}$ components of the microwave fields. If the $\sigma^{\pm}$ components are balanced, shifts will largely cancel. More generally, ac Zeeman shifts will result in a clock shift of

$$\delta = \frac{(\Delta_{1,7} + \Delta_{1,8})\tau_1 + (\Delta_{2,6} + \Delta_{2,7})\tau_2}{3(T + \tau_1 + \tau_2)}, \tag{9}$$

where $\Delta_{k,F}$ is the ac Zeeman shift of $|F\rangle$ when Ω_k is applied. This shift has a similar form as that from a probe-induced ac Stark shift when using Ramsey spectroscopy. Consequently, autobalanced Ramsey spectroscopy would simultaneously eliminate both optical probe- and microwave-induced shifts [18,19]. For this experiment, we measured the π times for all $\Delta m = 0, \pm 1$ transitions from $|7\rangle$ and the results are tabulated in Table I. Values given are accurate to ~5%. Scaling the results to the 10 ms π times used in this experiment, we estimate the shift from Eq. (9) to be $\sim 2 \times 10^{-20}$ relative to the clock frequency. A similar type of shift would also arise if the Ramsey times are not properly balanced, but this is unlikely to be significant in practice.

Our demonstration has been implemented on the $|^1S_0, 7, 1\rangle \leftrightarrow |^3D_1, 7, 0\rangle$ transition due to practical considerations of our current laser set up. However, the technique can be applied starting from any upper F level, with an appropriate change to the microwave offset $\bar{\omega}'_{\bar{F}}$. Starting from the upper $F = 8$ level, for example, would allow the $|^1S_0, 7, 0\rangle \leftrightarrow |^3D_1, 8, 0\rangle$ transition to be used eliminating the linear Zeeman sensitivity of the ground state. This leaves only the quadratic Zeeman shifts of the upper $m = 0$ states with estimated sensitivities of 2.27, −0.12, and −2.15 mHz/μT^2 for $|6\rangle$, $|7\rangle$, and $|8\rangle$, respectively, and just −4.7 μHz/μT^2 for the hyperfine-averaged clock frequency [20]. Such sensitivities require rather modest experimental control of spatial and temporal variations of the ambient magnetic field, even for the long interrogation times made possible with current laser technology.

TABLE I. Measured π times for transitions $|^3D_1, 7, 0\rangle \leftrightarrow |^3D_1, F, m\rangle$ for $F = 6$, 8 and $m = 0, \pm 1$; π times for transitions $|^3D_1, 7, \pm 1\rangle \leftrightarrow |^3D_1, F, 0\rangle$ can be determined by scaling with appropriate Clebsch-Gordan coefficients.

Transition	$m = -1$	$m = 0$	$m = 1$
$F = 6$	7 ms	3.5 ms	9 ms
$F = 8$	23 ms	3.5 ms	20 ms

Note that the differential shift between the outer and inner ions is almost completely determined by the quadrupole shift induced by the neighboring ions: axial micromotion contributes at the few mHz level and all static trapping fields appear common mode to the ions. Consequently, the observed frequency differences in Figs. 2(a) and 2(b) can provide a reasonable estimate of the quadrupole moment. From [8], the quadrupole contribution to the frequency difference in Fig. 2(a) is given by,

$$h\Delta f = \frac{14}{25}(3\cos^2\theta - 1)\Theta(^3D_1)\frac{m\omega_z^2}{e}, \tag{10}$$

where e is the elementary charge, m is the mass of the ion, θ is the angle between the applied dc magnetic field and trap axis, and ω_z is the axial trap frequency. In this expression, the value of $\Theta(^3D_1)$ is specified in accordance with the definition given in [14]. Using the measured trap frequency of $\omega_z = 2\pi \times 131.66(1)$ kHz, a micromotion contribution of 4.7(2) mHz inferred from Raman sideband spectroscopy, and allowing $|\theta| < 5°$, gives an estimated quadrupole moment of $\Theta(^3D_1) = 0.634(9)ea_0^2$ where a_0 is the Bohr radius. This value is comparable to the theoretical estimate of $\Theta(^3D_1) = 0.655ea_0^2$ given in [21], taking into account their choice of convention and omitted sign.

In summary, we have proposed and demonstrated a simple technique to effect hyperfine averaging during Ramsey interrogation of a $^{176}Lu^+$ clock transition. The technique can be viewed as a form of dynamic decoupling, which eliminates dominant sources of inhomogeneous broadening in a multi-ion clock implementation. The level of suppression demonstrated is limited by the maximum differential quadrupole shift and interrogation time currently achievable. Even with this limitation, we expect tensor shifts to be suppressed well below 10^{-18} when using the technique in conjunction an optimal field alignment as demonstrated in [8].

The implementation can be readily adapted so as to utilize only $m = 0$ states providing improved resilience against magnetic field noise. At our current operating field of ~0.1 mT, component $m = 0$ states involved in the interrogation are two orders of magnitude less sensitive to magnetic field noise compared to the stretch states used in Al^+, for example. This is an important practical consideration for achieving long interrogation times. In addition, the technique is compatible with autobalanced Ramsey spectroscopy, so that probe induced ac Stark shifts can also be eliminated [18,19].

We have also provided a straightforward means to measure the quadrupole moment for the $^3D_1$ level utilizing the differential quadrupole shift induced by neighboring ions. All applied static electric fields including stray fields appear in common mode so that the characterization of these fields is unnecessary. Our current estimate is limited

by the ability to characterize the angle of the magnetic field with respect to the ion crystal and a small amount of axial micromotion. Alignment of the field could be improved by maximizing the tensor shift with respect to bias coil currents and micromotion diminished by increasing the axial confinement and lowering the rf drive voltage. We anticipate that an order of magnitude improvement in the measurement precision should be possible with these improvements.

We thank Ravid Shaniv for many helpful discussions. This work is supported by the National Research Foundation, Prime Ministers Office, Singapore and the Ministry of Education, Singapore under the Research Centres of Excellence programme. This work is also supported by A*STAR SERC Public Sector Research Funding (PSF) Grant (SERC Project No. 1521200080). T. R. acknowledges support from the Lee Kuan Yew postdoctoral fellowship.

*phybmd@nus.edu.sg

[1] A. D. Ludlow, M. M. Boyd, J. Ye, E. Peik, and P. O. Schmidt, Optical atomic clocks, Rev. Mod. Phys. **87**, 637 (2015).

[2] T. L. Nicholson, S. L. Campbell, R. B. Hutson, G. E. Marti, B. J. Bloom, R. L. McNally, W. Zhang, M. D. Barrett, M. S. Safronova, G. F. Strouse *et al.*, Systematic evaluation of an atomic clock at 2×10^{-18} total uncertainty, Nat. Commun. **6**, 6896 (2015).

[3] W. F. McGrew, X. Zhang, R. J. Fasano, S. A. Schäffer, K. Beloy, D. Nicolodi, R. C. Brown, N. Hinkley, G. Milani, M. Schioppo *et al.*, Atomic clock performance enabling geodesy below the centimetre level, Nature (London) **564**, 87 (2018).

[4] C.-w. Chou, D. B. Hume, J. C. J. Koelemeij, D. J. Wineland, and T. Rosenband, Frequency Comparison of Two High-Accuracy Al^+ Optical Clocks, Phys. Rev. Lett. **104**, 070802 (2010).

[5] N. Huntemann, C. Sanner, B. Lipphardt, C. Tamm, and E. Peik, Single-Ion Atomic Clock with 3×10^{-18} Systematic Uncertainty, Phys. Rev. Lett. **116**, 063001 (2016).

[6] M. D. Barrett, Developing a field independent frequency reference, New J. Phys. **17**, 053024 (2015).

[7] K. J. Arnold, R. Kaewuam, A. Roy, T. R. Tan, and M. D. Barrett, Blackbody radiation shift assessment for a lutetium ion clock, Nat. Commun. **9**, 1650 (2018).

[8] T. R. Tan, R. Kaewuam, K. J. Arnold, S. R. Chanu, Z. Zhang, M. Safronova, and M. D. Barrett, Suppressing Inhomogeneous Broadening in a Lutetium Multi-Ion Optical Clock, Phys. Rev. Lett. **123**, 063201 (2019).

[9] C. Sanner, N. Huntemann, R. Lange, C. Tamm, E. Peik, M. S. Safronova, and S. G. Porsev, Optical clock comparison for Lorentz symmetry testing, Nature (London) **567**, 204 (2019).

[10] K. Pyka, N. Herschbach, J. Keller, and T. E. Mehlstäubler, A high-precision segmented paul trap with minimized micromotion for an optical multiple-ion clock, Appl. Phys. B **114**, 231 (2014).

[11] K. Arnold, E. Hajiyev, E. Paez, C. H. Lee, M. D. Barrett, and J. Bollinger, Prospects for atomic clocks based on large ion crystals, Phys. Rev. A **92**, 032108 (2015).

[12] R. Shaniv, N. Akerman, T. Manovitz, Y. Shapira, and R. Ozeri, Quadrupole Shift Cancellation Using Dynamic Decoupling, Phys. Rev. Lett. **122**, 223204 (2019).

[13] P. Dubé, A. A. Madej, Z. Zhou, and J. E. Bernard, Evaluation of systematic shifts of the $^{88}Sr^+$ single-ion optical frequency standard at the 10^{-17} level, Phys. Rev. A **87**, 023806 (2013).

[14] W. M. Itano, External-field shifts of the $^{199}Hg^+$ optical frequency standard, J. Res. Natl. Inst. Stand. Technol. **105**, 829 (2000).

[15] J. Keller, D. Kalincev, T. Burgermeister, A. P. Kulosa, A. Didier, T. Nordmann, J. Kiethe, and T. E. Mehlstäubler, Probing Time Dilation in Coulomb Crystals in a High-Precision Ion Trap, Phys. Rev. Applied **11**, 011002 (2019).

[16] M. Chwalla, K. Kim, T. Monz, P. Schindler, M. Riebe, C. F. Roos, and R. Blatt, Precision spectroscopy with two correlated atoms, Appl. Phys. B **89**, 483 (2007).

[17] C.-W. Chou, D. B. Hume, M. J. Thorpe, D. J. Wineland, and T. Rosenband, Quantum Coherence Between Two Atoms Beyond $Q = 10^{15}$, Phys. Rev. Lett. **106**, 160801 (2011).

[18] C. Sanner, N. Huntemann, R. Lange, C. Tamm, and E. Peik, Autobalanced Ramsey Spectroscopy, Phys. Rev. Lett. **120**, 053602 (2018).

[19] V. I. Yudin, A. V. Taichenachev, M. Yu Basalaev, T. Zanon-Willette, J. W. Pollock, M. Shuker, E. A. Donley, and J. Kitching, Generalized Autobalanced Ramsey Spectroscopy of Clock Transitions, Phys. Rev. Applied **9**, 054034 (2018).

[20] E. Paez, K. J. Arnold, E. Hajiyev, S. G. Porsev, V. A. Dzuba, U. I. Safronova, M. S. Safronova, and M. D. Barrett, Atomic properties of Lu^+, Phys. Rev. A **93**, 042112 (2016).

[21] S. G. Porsev, U. I. Safronova, and M. S. Safronova, Clock-related properties of Lu^+, Phys. Rev. A **98**, 022509 (2018). The quadrupole moments given use a nuclear physics convention, which includes an extra factor of two. For consistency with notation used here and in [14], they must be multiplied by $-1/2$.